Observational Constraints on the Cloud Feedback Pattern Effect

Timothy A. Myers,[a,b,c] Mark D. Zelinka,[c] Stephen A. Klein,[c]

[a] *Cooperative Institute for Research in Environmental Sciences (CIRES), University of Colorado, Boulder, Colorado*

[b] *Physical Science Laboratory, National Oceanic and Atmospheric Administration, Boulder, Colorado*

[c] *Lawrence Livermore National Laboratory, Livermore, California*

Corresponding author: Timothy A. Myers, timothy.myers@noaa.gov

Early Online Release: This preliminary version has been accepted for publication in *Journal of Climate*, may be fully cited, and has been assigned DOI 10.1175/JCLI-D-22-0862.1. The final typeset copyedited article will replace the EOR at the above DOI when it is published.

ABSTRACT: Model evidence for the "pattern effect" assumes that global climate models (GCMs) faithfully simulate how clouds respond to varying sea-surface temperature (SST) patterns and associated meteorological perturbations. We exploit time-invariant satellite-based estimates of the sensitivity of marine low clouds to meteorological perturbations to estimate how these clouds responded to time-varying SST patterns and meteorology between 1870 and 2014. GCMs and reanalyses provide estimates of the historical meteorological changes. Observations suggest that increasing estimated inversion strength (EIS) between 1980 and 2014 produced a negative low cloud feedback, opposite to the positive feedback expected from increasing CO_2. This indicates that the processes responsible for marine cloud changes from 1980 to near-present are distinct from those associated with an increase in CO_2. We also observationally constrain the difference between the historical near-global marine low cloud feedback, λ_{cloud}^{hist}, and that arising from increasing CO_2, λ_{cloud}^{4xCO2}. We find that this *cloud feedback pattern effect* depends strongly on time period and reanalysis dataset, and that varying changes in EIS and SST with warming explain much of its variability. Between 1980 and 2014, we estimate that $\lambda_{cloud}^{4xCO2} - \lambda_{cloud}^{hist}$ =0.78±0.21 W m^{-2} K^{-1} (90% confidence) assuming meteorological changes from the Multiple-Reanaysis Ensemble, implying a total pattern effect (that arising from all climate feedbacks) of 1.86±0.45 W m^{-2} K^{-1}. This observational evidence corroborates previous quantitative estimates of the pattern effect, which heretofore relied largely upon GCM-based cloud changes. However, disparate historical meteorological changes across individual reanalyses contribute to considerable uncertainty in its magnitude.

Accepted for publication in *Journal of Climate.* DOI 10.1175/JCLI-D-22-0862.1.

1. Introduction

Clouds produce strong interannual-to-interdecadal variations in the radiative fluxes entering and exiting the Earth's surface and atmosphere (Andrews et al. 2018, 2022; Ceppi and Fueglistaler 2021; Fueglistaler 2019; Gregory and Andrews 2016; Loeb et al. 2018, 2020; Myers et al. 2018; Silvers et al. 2018; Zhou et al. 2016). These variations are assoicated with feedbacks that modify the climate's radiative damping rate, acting to amplify or dampen global mean temperature change. For example, satellite observations reveal that a positive shortwave cloud feedback accelerated the rate of global mean temperature increase in the years following the "hiatus" of the warming rate in the early 2000s (Loeb et al. 2018). The "hiatus", on the other hand, has been linked to a negative shortwave cloud feedback (Zhou et al. 2016) driven by an increase in stratocumulus cloud coverage over the eastern Pacific Ocean between the 1980s and 2000s (Clement et al. 2009; Norris and Evan 2015; Seethala et al. 2015).

Atmosphere-only global climate model (GCM) simulations suggest that fluctuating SST patterns produced interdecadal changes in global radiative and cloud feedbacks over the last ~100 years, including the negative cloud feedback between the 1980s and 2000s (Andrews et al. 2018, 2022; Dong et al. 2021; Gregory and Andrews 2016; Zhou et al. 2016). These changes are hypothesized to be due to fluctuating Pacific SST patterns and associated variations in stratocumulus cloud coverage. Warming in the western tropical Pacific relative to the eastern tropical Pacific between the 1980s and 2000s likely resulted in an increase in lower tropospheric stability throughout the tropics. This increased the inversion strength capping eastern Pacific stratocumulus clouds, increasing their coverage, producing a negative feedback to planetary warming (Andrews and Webb 2018; Cesana and Del Genio 2021; Seethala et al. 2015; Zhou et al. 2016).

Notably, marine low cloud feedbacks associated with increasing CO_2 in GCMs, large-eddy simulations, and as constrained by observations are positive (Ceppi and Nowack 2021; Cesana and Del Genio 2021; Myers et al. 2021; Sherwood et al. 2020; Zelinka et al. 2020). The difference between CO_2-induced global climate feedbacks and those that have occurred historically is what has been called the "pattern effect", since it is the distinct SST patterns between the two scenarios that explain their differing feedbacks and inferred climate sensitivities (Sherwood et al. 2020).

Model evidence for the pattern effect assumes that GCMs realistically simulate how clouds respond to varying SST patterns and associated meteorological perturbations. In this study, we

Accepted for publication in *Journal of Climate.* DOI 10.1175/JCLI-D-22-0862.1.

exploit time-invariant satellite-based estimates of the sensitivity of marine low clouds to meteorological perturbations (Scott et al. 2020) to quantify how these clouds responded to time-varying SST patterns and meteorology between 1870 and 2014. GCMs and reanalyses provide estimates of the historical meteorological changes. Moreover, using recently developed observational constraints on the low cloud feedback associated with increasing CO_2 (Myers et al. 2021), we also quantify the difference between our historical feedback estimates and the CO_2-induced feedback. These estimates provide quantitative observational constraints on what we call the *cloud feedback pattern effect*, which, as we will show, provides further constraints on the pattern effect arising from all climate feedbacks. Based on such constraints, we are able to assess GCM-based estimates of the pattern effect. Our study is unique insofar as we provide quantitative estimates of the pattern effect without relying on GCM simulations of cloud changes, unlike most previous estimates (Andrews et al. 2018, 2022; Sherwood et al. 2020).

2. Data and Methods

a. Observational constraints

1) Framework

Table 1 provides a summary of the observationally constrained marine low cloud feedback estimates computed in this study. We follow a modified version of the methodology developed by Myers et al. (2021) to observationally constrain how marine low clouds have changed in response to varying historical SST patterns and large-scale meteorological conditions. To do so, we introduce a time-varying component to the cloud-controlling factors (CCFs) x_i of equation (1) of Myers et al. (2021), who did not explicitly consider how variations in CCFs may depend on time period. Then, a Taylor series approximation of the time-varying sensitivity of low cloud-induced radiative flux R at the top of the atmosphere to changes in global mean surface temperature T_g, or λ_{cloud}, is given as

$$\lambda_{cloud} = \frac{dR(\theta,\phi,t)}{dT_g} = \sum_i \frac{\partial R(\theta,\phi)}{\partial x_i} \frac{dx_i(\theta,\phi,t)}{dT_g}, \tag{1}$$

Accepted for publication in *Journal of Climate.* DOI 10.1175/JCLI-D-22-0862.1.

Table 1. Observationally constrained marine low cloud feedback estimates calculated in this study. Note that the feedback from increasing CO_2 is reproduced from Myers et al. (2021).

Dataset for Meteorological Changes $dx_i(\theta,\phi,t)/dT_g$	**Dataset for *Meteorological Cloud Radiative Kernels*** $\partial R(\theta,\phi)/\partial x_i$	**Feedback Type**
AMIP-piForcing (six CMIP6 models)	MODIS/CERES or ISCCP/PATMOS-x	response to SST patterns
reanalyses (seven choices)		historical
abrupt4xCO2 (7 CMIP5 and 11 CMIP6 models)		response to increasing CO_2

where θ is latitude, ϕ is longitude, and t is time. The x_i include sea surface temperature (SST), estimated inversion strength (EIS), horizontal surface temperature advection (Tadv), relative humidity at 700 hPa (RH_{700}), vertical velocity at 700 hPa (ω_{700}), and near-surface wind speed (WS). EIS and Tadv are computed as described in Myers and Norris (2015). We note that our method does not consider changes in low clouds driven by aerosols alone (as in e.g. Wall et al. (2022)). Nonetheless, cloud changes arising from aerosol-induced perturbations in CCFs are included in our approach.

The $\partial R(\theta,\phi)/\partial x_i$ correspond to the observation-based *meteorological cloud radiative kernels* developed by Scott et al. (2020) and applied in Myers et al. (2021); each $\partial R(\theta,\phi)/\partial x_i$ quantifies the local interannual sensitivity of R to a perturbation in x_i when all other $x_{i\neq j}$ are held fixed. These sensitivites are assumed to be time-invariant, which is further discussed in Section 2.a.6.

Each $dx_i(\theta,\phi,t)/dT_g$ represents the local response of x_i to climate warming within some time period centered at time t. This term is responsible for any temporal dependence of λ_{cloud}.

In the next two subsections, we describe how we compute $\partial R(\theta,\phi)/\partial x_i$ and $dx_i(\theta,\phi,t)/dT_g$ to ultimately produce historical estimates of λ_{cloud}.

2) Meteorological cloud radiative kernels

At each $5^\circ \times 5^\circ$ latitude-longitude oceanic grid box between 60° S and 60° N, the $\partial R(\theta,\phi)/\partial x_i$ are estimated as the multi-linear regression coefficients that result from regressing the time series of deseasonalized and detrended interannual monthly anomalies in satellite-derived R onto anomalies in x_i from a reanalysis and a standard SST dataset. See Myers et al. (2021) and Scott et al. (2020) for details.

Accepted for publication in *Journal of Climate.* DOI 10.1175/JCLI-D-22-0862.1.

The observational low-cloud-induced radiative flux anomalies in R at the top of the atmosphere are computed as described in Myers et al. (2021) (e.g. their equation (2)) and Scott et al. (2020)). Note that the radiative anomalies are exclusively due to changes in non-obscured low-level clouds and not due to changes in the obscuration of low clouds by higher-level clouds. Radiative fluxes are derived using July 2002 to December 2018 data from the Moderate Resolution Imaging Spectroradiometer (MODIS) collection 6.1 and from the Clouds and the Earth's Radiant Energy System (CERES) Flux-by-Cloud-Type (FBCT) dataset and using July 1983 to June 2002 data from the International Satellite Cloud Climatology Project (ISCCP) H-series and from the Pathfinder Atmospheres Extended data record (PATMOS-x) (Pincus et al. 2012; Sun et al. 2022; Young et al. 2018; Heidinger et al. 2014).

We apply two independent sets of observational $\partial R(\theta, \phi)/\partial x_i$. One set is derived from July 2002 to December 2018 MODIS-estimated anomalies in R averaged with those from CERES-FBCT, and the other set is derived from July 1983 to June 2002 ISCCP-estimated anomalies in R averaged with those from PATMOS-x. We consider the two sets of *meteorological cloud radiative kernels* to be independent since they are derived from different satellite observing systems and time periods.

3) Historical changes in meteorology

We compute each $dx_i(\theta, \phi, t)/dT_g$ in equation (1) at a $5^\circ \times 5^\circ$ spatial scale over various multi-decadal periods. These changes in CCFs are estimated from two different data sources: i) output from atmosphere-only GCMs forced by historical variations in SST and ii) an ensemble of atmospheric reanalyses. We choose periods that are 35 years long based on the time length of overlap between GCM output and reanalysis data.

The GCM output is from the *AMIP-piForcing* experiments of the Coupled Model Intercomparison Project phase 6 (CMIP6) (Eyring et al. 2016; Webb et al. 2017). These are 1870-2014 atmosphere-only simulations forced by historical variations in SST and sea ice, with greenhouse gas and aerosol forcing agents held fixed at pre-industrial levels. SST and sea ice are specified by the Atmospheric Model Intercomparison Project (AMIP) II boundary condition data set (Gates et al. 1999; Hurrell et al. 2008; Taylor et al. 2000). AMIP II uses HadISST1 SST (Rayner et al. 2003) before November 1981 and version 2 of the National Oceanic and Atmospheric Administration (NOAA) weekly optimum interpolation (OI.v2) SST analysis (Reynolds et al. 2002) afterward. Using the GCMs,

Accepted for publication in *Journal of Climate.* DOI 10.1175/JCLI-D-22-0862.1.

we compute each $dx_i(\theta,\phi,t)/dT_g$ across sliding 35-yr windows via a centered finite differencing method, described as follows. For each 35-yr window, we composite the annual mean anomalies of the CCFs on T_g. We then take the mean composite difference in x_i between the subset of data corresponding to above-median T_g and the subset corresponding to below-median T_g, divided by the difference in mean anomalies in T_g between these two subsets. Finally, we compute the ensemble mean $dx_i(\theta,\phi,t)/dT_g$ across six CMIP6 models (Supplementary Table 1) to produce a central best estimate. The $dx_i(\theta,\phi,t)/dT_g$ computed using linear regression are very similar to those computed using the finite differencing method. The advantage of the latter relative to the former method is computational ease, a reduced sensitivity to outliers, and a simplified computation of uncertainty.

The atmospheric reanalysis data for estimating $dx_i(\theta,\phi,t)/dT_g$ are from seven different products and include the: Climate Forecast System Reanalysis (CFSR; Saha et al. (2010)), the Interim European Centre for Medium-Range Weather Forecasts (ECMWF) Re-Analysis (ERA- Interim; Dee et al. (2011)), fifth generation of the ECMWF atmospheric reanalysis of the global climate (ERA5; Hersbach et al. (2020)), Japanese 55-year Reanalysis Project (JRA-55; Ebita et al. (2011)), Modern-Era Retrospective Analysis for Research and Applications (MERRA; Rienecker et al. (2011)), MERRA version 2 (MERRA-2; Gelaro et al. (2017)), and the Collaborative REAnalysis Technical Environment - Multiple Reanalysis Ensemble v3 (CREATE-MRE3; Potter et al. (2018)). The Multiple Reanalysis Ensemble (MRE) represents an ensemble mean across the six other source reanalysis datasets. Therefore, we consider it to be among the most realistic of the reanalyses examined here, along with ERA5, which is widely considered to be the most state-of-the-art reanalysis product. Although more directly observed data for estimating $dx_i(\theta,\phi,t)/dT_g$ exists, we examine CCF changes from reanalyses so that any large-scale changes within a given reanalysis are dynamically consistent.

For each reanalysis, the centered finite differencing method for computing $dx_i(\theta,\phi,t)/dT_g$ described above is applied to a single 1980-2014 period, corresponding to the period of overlapping data availability across reanalyses and GCMs. T_g from ERA5 is used in all reanalysis-based calculations to eliminate the effects of differences in planetary warming rates across reanalyses. ω_{700} data are unavailable for JRA55 and the MRE, so for these two datasets we use changes in the five other CCFs to compute observationally-constrained feedbacks given by equation (1). However, feedback components due to changes in ω_{700} from the available reanalyses are small.

Accepted for publication in *Journal of Climate.* DOI 10.1175/JCLI-D-22-0862.1.

We note that the meteorological changes estimated from reanalyses may have contributions from greenhouse gas and aerosol forcing agents that are independent of global mean surface temperature, which could lead to cloud adjustments that contaminate our estimates of cloud feedback (e.g. Kamae et al. (2015); Qu et al. (2015); Zhou et al. (2021)). By design, these meteorological changes are excluded in the *AMIP-piForcing* experiments, motivating their use to examine cloud feedbacks. Hence, a portion of differences in cloud feedbacks between the reanalysis-based and *AMIP-piForcing*-based estimates may be attributable to cloud adjustments to greenhouse gas and aerosol forcing agents.

4) Feedback from increasing CO_2

To compare historical low cloud feedbacks to those arising from increasing CO_2, we also reproduce the method of Myers et al. (2021) to compute observational constraints on low cloud feedbacks associated with an instantaneous quadrupling of atmospheric CO_2. Put simply, these feedbacks are calculated by convolving the *meteorological cloud radiative kernels* with long-term changes in CCFs simulated by GCMs in the *abrupt4xCO2* experiment. Following Myers et al. (2021), $dx_i(\theta,\phi,t)/dT_g$ is then computed as the difference in mean x_i divided by the difference in mean T_g between years 1–20 and 121–140 of the *abrupt4xCO2* experiment, and averaged over the 7 CMIP5 and 11 CMIP6 models specified in that study.

5) Uncertainty

90% confidence intervals of the observationally-constrained cloud feedbacks are computed following the method of Myers et al. (2021). The uncertainty ranges consider both imperfect observational estimates of the *meteorological cloud radiative kernels* and imperfect estimates of historical or future changes in CCFs. To compute the total uncertainty of the feedback for a given 35-yr period from the *AMIP-piForcing* experiments, we add the uncertainty arising from $\partial R(\theta,\phi)/\partial x_i$ in quadrature with the uncertainty arising from $dx_i(\theta,\phi,t)/dT_g$. A slight modification compared to Myers et al. (2021) is that to compute uncertainty arising from $dx_i(\theta,\phi,t)/dT_g$ for a given 35-yr period, we consider the full range of feedbacks computed using individual $dx_i(\theta,\phi,t)/dT_g$ across the six GCMs, instead of estimating the 5 - 95 percentile range. This choice is based on the limited

Accepted for publication in *Journal of Climate.* DOI 10.1175/JCLI-D-22-0862.1.

sample of GCMs examined, which corresponds to those providing the ISCCP simulator output from the *AMIP-piForcing* experiments (Bodas-Salcedo et al. 2011).

An uncertainty that we do not consider is the dependence of the CCFs on the underlying SST dataset used in the GCM simulations. In light of previous findings that the pattern effect and the historical tropical Pacific SST pattern depend on SST dataset (Andrews et al. 2022; Silvers and Fueglistaler 2021; Modak and Mauritsen 2022), we expect that historical estimates of CCFs will exhibit a similar dependence. Simulations to quantify this dependence are not readily available, so we leave this as a topic for future work.

6) Caveats

Our framework to compute cloud feedbacks assumes that the observational estimates of $\partial R(\theta,\phi)/\partial x_i$ are time-invariant and that the model or reanalysis estimates of $dx_i(\theta,\phi,t)/dT_g$ for the historical period and response to increasing CO_2 are realistic. The first assumption was justified by Myers et al. (2021), who showed that the CCF framework was able to predict an out-of-sample marine heatwave and that their feedback estimates were largely insensitive to the time period used for computing $\partial R(\theta,\phi)/\partial x_i$. Evidence for the time-invariance assumption is also discussed critically by Klein et al. (2017). The second assumption is more difficult to assess. We partially deal with uncertainty of $dx_i(\theta,\phi,t)/dT_g$ by considering output from a set of structurally diverse GCMs and by considering a set of structurally diverse reanalyses. The uncertainty around how CCFs change with planetary warming is related to the uncertainty at the heart of the pattern effect - why the pattern of Pacific SST change since ~1980 does not resemble the SST response to increasing CO_2 predicted by fully coupled GCMs. There are several contending hypotheses addressing this uncertainty that we do not attempt to rigorously assess here (Hartmann 2022; Heede and Fedorov 2021; Kostov et al. 2018; Rye et al. 2020; Seager et al. 2019; Sherwood et al. 2020; Watanabe et al. 2021; Wills et al. 2022). If model predictions of changes in SST patterns and CCFs with increasing CO_2 are systematically biased, our cloud feedback and pattern effect estimates will be similarly biased. But our framework is meant to reduce the uncertainty surrounding the response of clouds to large-scale forcing, not the uncertainty of the large-scale forcing itself. Given these caveats and assumptions, we expect that the true uncertainty of our cloud feedback and pattern effect estimates is larger than what we quantify.

Accepted for publication in *Journal of Climate.* DOI 10.1175/JCLI-D-22-0862.1.

Finally, we emphasize that our approach is not purely observational, given that changes in CCFs are provided by GCMs and reanalyses. Nonetheless, our estimates exploit observation-based *meteorological cloud radiative kernels* to constrain the response of clouds to simulated historical and future changes in CCFs, thereby providing observational constraints on cloud feedbacks on multiple timescales.

b. GCM Feedbacks

We also examine historical low cloud feedbacks simulated by six CMIP6 models (Supplementary Table 1) in the *AMIP-piForcing* experiments to compare to our observationally constrained estimates. These correspond to those models providing ISCCP simulator output for these simulations as well as for the *abrupt4xCO2* experiments, with one exception. For a given 35-yr period, these are computed by dividing annual mean anomalies of R into subsets above and below the median T_g. The feedbacks, $dR(\theta,\phi,t)/dT_g$, are then calculated as the difference in mean anomalies in R divided by the difference in mean anomalies in T_g between these two subsets. Anomalies of R for the models are computed by applying the cloud radiative kernels of Zelinka et al. (2012) to interannual monthly anomalies in non-obscured low-level cloud fraction from the ISCCP simulator output, following equation (2) of Myers et al. (2021).

Lastly, we examine low cloud feedbacks simulated by the same six CMIP6 models in the *abrupt4xCO2* experiments. With the exception of one model, these are computed following Myers et al. (2021). For the other model (CESM2), we compute the low cloud feedback using the approach of Webb et al. (2006) owing to a lack of ISCCP simulator output for this model's *abrupt4xCO2* run. The Supporting Information of Zelinka et al. (2020) provides details of this calculation.

3. Results

a. Estimating historical changes in low clouds

We begin by highlighting the utility of our methodology for predicting historical variations in low clouds. Modifying equation (1) to replace $dx_i(\theta,\phi,t)/dT_g$ with annual mean anomalies of x_i from the *AMIP-piForcing* experiments permits quantification of cloud radiative anomalies between 1870 and 2014. Figure 1 shows the time series of annual mean near-global marine low cloud radiative anomalies constrained in this way and the time series of EIS anomalies from the *AMIP-piForcing*

Accepted for publication in *Journal of Climate.* DOI 10.1175/JCLI-D-22-0862.1.

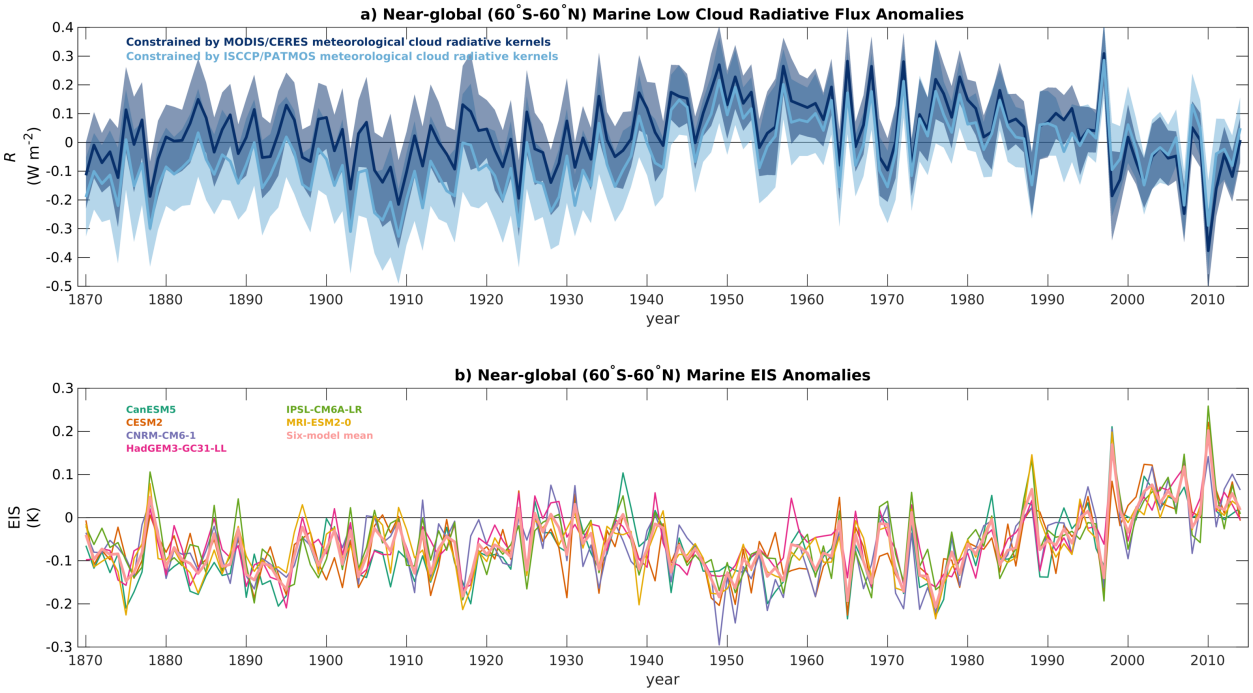

FIG. 1. Annual mean (a) near-global marine low cloud radiative anomalies constrained by satellite observations and changes in CCFs from the *AMIP-piForcing* experiments, computed using a modified version of equation (1) (as described in main text), and (b) EIS anomalies from the *AMIP-piForcing* experiments. The dark blue line in (a) corresponds to the estimate constrained by MODIS- and CERES-derived *meteorological cloud radiative kernels*, while the light blue line corresponds to the estimate constrained by ISCCP- and PATMOS-x-derived *meteorological cloud radiative kernels*. Shading around observationally-constrained estimates span 90% confidence intervals. Radiative anomalies are scaled by planetary fractional area.

experiments. Here and throughout the paper, anomalies are defined with respect to the 1981-2010 climatology. The marine cloud (Fig. 1a) and EIS (Fig. 1b) anomalies exhibit substantial variability, and in the last several decades EIS has increased in tandem with a cooling cloud radiative effect over the oceans. This implicates patterns of SST change as a driver of historical marine cloud and EIS changes and motivates our formal feedback analysis that follows in the rest of the paper.

b. Spatially resolved low cloud feedback on two time timescales

Figure 2 shows estimates of historical marine low cloud feedbacks constrained by MODIS and CERES along with 1980-2014 changes in CCFs from ERA5 (Fig. 2a), the Multi-reanalysis

Accepted for publication in *Journal of Climate*. DOI 10.1175/JCLI-D-22-0862.1.

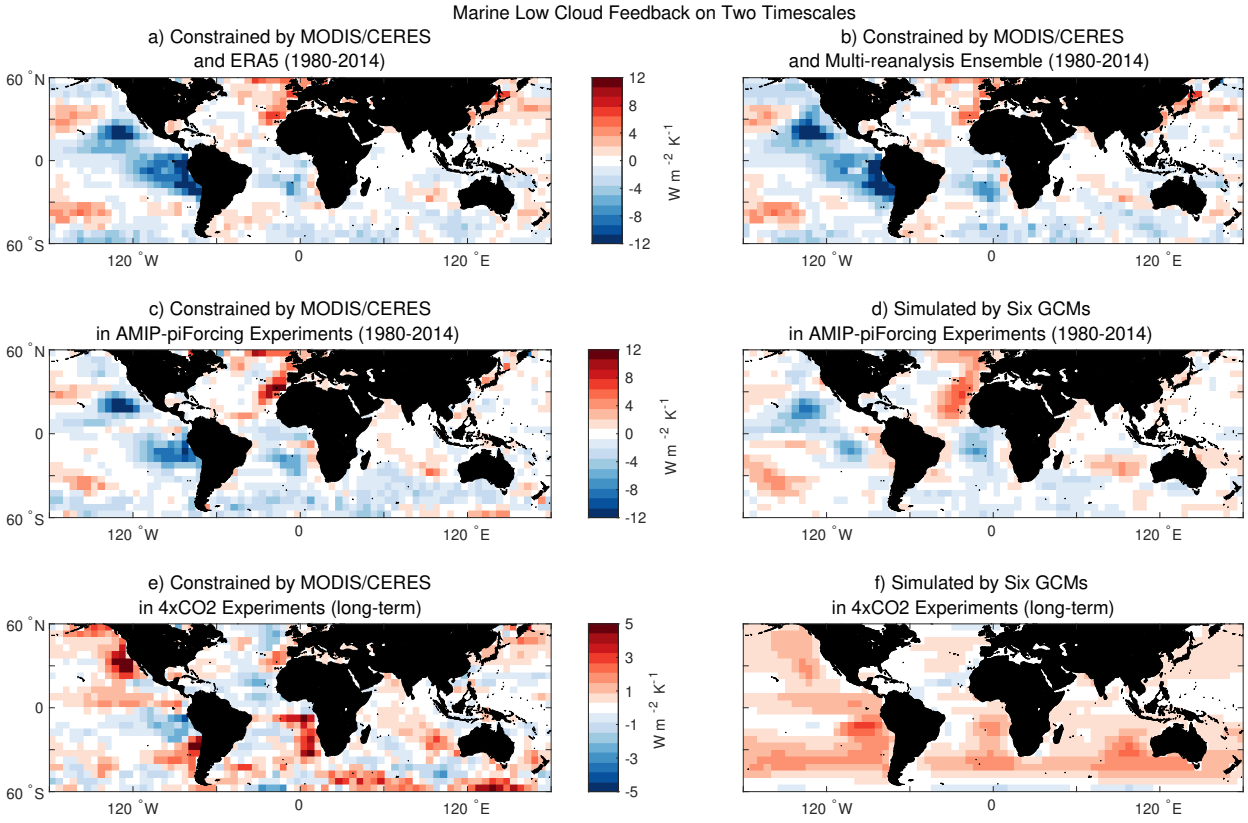

FIG. 2. Historical marine low cloud feedback constrained by MODIS- and CERES-derived *meteorological cloud radiative kernels* along with 1980-2014 changes in CCFs from (a) ERA5, (b) the Multi-reanalysis Ensemble, and (c) output from the *AMIP-piForcing* experiments. (d) Historical marine low cloud feedback simulated by six CMIP6 models in the *AMIP-piForcing* experiments. Long-term marine low cloud feedbacks arising from increasing CO_2 (e) as constrained by MODIS- and CERES-derived *meteorological cloud radiative kernels* and (f) as simulated by six CMIP6 models. Note the different color scale range in (e) and (f).

Ensemble (Fig. 2b), and the *AMIP-piForcing* experiments (Fig. 2c). The two reanalysis-based estimates are very similar and exhibit strong negative feedbacks in the stratocumulus regions over the eastern subtropical Pacific Ocean, with weaker and more variable feedbacks elsewhere. This pattern is qualitatively consistent with the increase in eastern subtropical Pacific low-level cloud fraction detected in the ISCCP D-series and PATMOS-x passive satellite datasets corrected for spurious variability and increase in total cloud fraction over the same region detected in surface observations between the 1980s and 2000s, which corroborates our method for constraining historical low cloud feedbacks (Clement et al. 2009; Norris and Evan 2015; Seethala et al. 2015).

Accepted for publication in *Journal of Climate*. DOI 10.1175/JCLI-D-22-0862.1.

The pattern of the observationally constrained feedback estimated using meteorological changes from the SST-driven simulations (Fig. 2c) is similar to that based on the reanalysis data and also resembles the historical feedback simulated by six CMIP6 models in the *AMIP-piForcing* experiments (Fig. 2d). This indicates that changes in marine clouds between 1980 and 2014 were driven by the particular pattern of SST change and the resulting variations in large-scale meteorological conditions. In particular, the dominant component of each of the historical feedback estimates constrained by observations is that due to EIS, which has robustly increased and induced a strong negative feedback over the eastern subtropical Pacific in recent decades (Supplementary Figs. 1-7), consistent with the findings of Zhou et al. (2016) and Cesana and Del Genio (2021). This increase in EIS in recent decades was likely a result of decreasing SST in tropical Pacific subsidence regions and increasing in SST in tropical Pacific ascent regions, from which warm free-tropospheric temperature anomalies were then propagated throughout the tropics (Zhou et al. 2016). This La Nina-like evolution is physically consistent with the observed acceleration of the tropical Pacific easterly trade winds in recent decades (1992-2011 in England et al. (2014) and 1979-2014 in Zhao and Allen (2019)), which may explain why changes in both Tadv and WS contribute as small negative low feedbacks in the eastern tropical Pacific in most of the reanalysis-based estimates (Supplementary Figs. 4 and 7).

Long-term marine low cloud feedbacks arising from increasing CO_2 as constrained by MODIS and CERES and as simulated by six CMIP6 models are shown in Fig. 2e and Fig. 2f, respectively. The main features of these observationally-constrained and GCM-simulated feedbacks are discussed extensively by Myers et al. (2021) and will not be reviewed further here. Of relevance to this study is the finding that both the observationally-constrained and model estimates reveal that the feedbacks from increasing CO_2 are, in general, more amplifying than the historical feedbacks. Major differences are seen over the eastern ocean stratocumulus regions, where the long-term feedback tends to be positive and the historical feedback tends to be negative. Smaller yet noticeable differences exist over portions of the extra-tropical North Pacific and southern oceans as well, where the long-term feedbacks also tend to be more amplifying than the historical feedbacks. Assuming that GCMs simulate realistic changes in CCFs with greenhouse warming, these findings suggest that estimates of historical marine low cloud feedbacks over recent decades cannot be used to infer the long-term feedbacks in response to increasing CO_2. This is further supported by the

Accepted for publication in *Journal of Climate.* DOI 10.1175/JCLI-D-22-0862.1.

lack of a clear relationship between the 1980-2014 *AMIP-piForcing* low cloud feedbacks and the *abrupt4xCO2* feedbacks simulated by the six GCMs examined here (Supplementary Fig. 8), in qualitative agreement with Andrews et al. (2022).

c. Temporal variations in low cloud feedback

How have low cloud feedbacks varied from the late 19th century to near-present? Figure 3a reveals a time-varying, near-global (60° S - 60° N), 35-yr low cloud feedback driven solely by varying historical SST patterns, with close alignment between the observational constraints and the ensemble mean of six CMIP6 models (Fig. 3a). This feedback has in-phase contributions from the tropics (35° S - 35° N; Fig. 3b) and midlatitudes (35° N/S - 60° N/S; Fig. 3c). The tropics provide the majority contribution to the variance in both observations and GCMs (Supplementary Fig. 9), although GCMs tend to overestimate its contribution. The near-global feedback has trended from positive to negative in recent decades, which is consistent with previous model results (Andrews et al. 2018, 2022; Gregory and Andrews 2016; Gregory et al. 2020; Zhou et al. 2016). The recent negative feedback is opposite to the positive long-term, near-global and tropical feedbacks from increasing CO_2 predicted by observational constraints and simulated by six CMIP6 models. Near-global feedbacks constrained by satellite observations and the meteorological changes from reanalyses are also negative. Hence, a negative near-global low cloud feedback likely occurred from the beginning of the satellite era to near-present, which is anomalous relative to the previous ~100 years and is inconsistent with the feedback associated with increasing CO_2.

Which CCFs are most responsible for temporal variations in the low feedback and its recent negative trend? Figure 4 shows that the trajectory of the near-global, tropical, and midlatitude marine low cloud feedbacks since the late 19th century closely follows that of the feedbacks induced by the evolution of EIS. Indeed, over each domain, the temporal covariance matrix among the feedback components normalized by the temporal variance in the total feedback itself reveals that EIS is the largest component of the variance (Supplementary Figs. 10 and 11). Changes in SST also induce a varying yet persistently positive feedback component at each spatial scale, in phase with that due to EIS. This positive SST-driven feedback component has decreased in recent decades, especially in the tropics, largely consistent with estimates from the reanalyses and as expected under the observed muted warming trend in the tropical Pacific. Overall, EIS and its

Accepted for publication in *Journal of Climate.* DOI 10.1175/JCLI-D-22-0862.1.

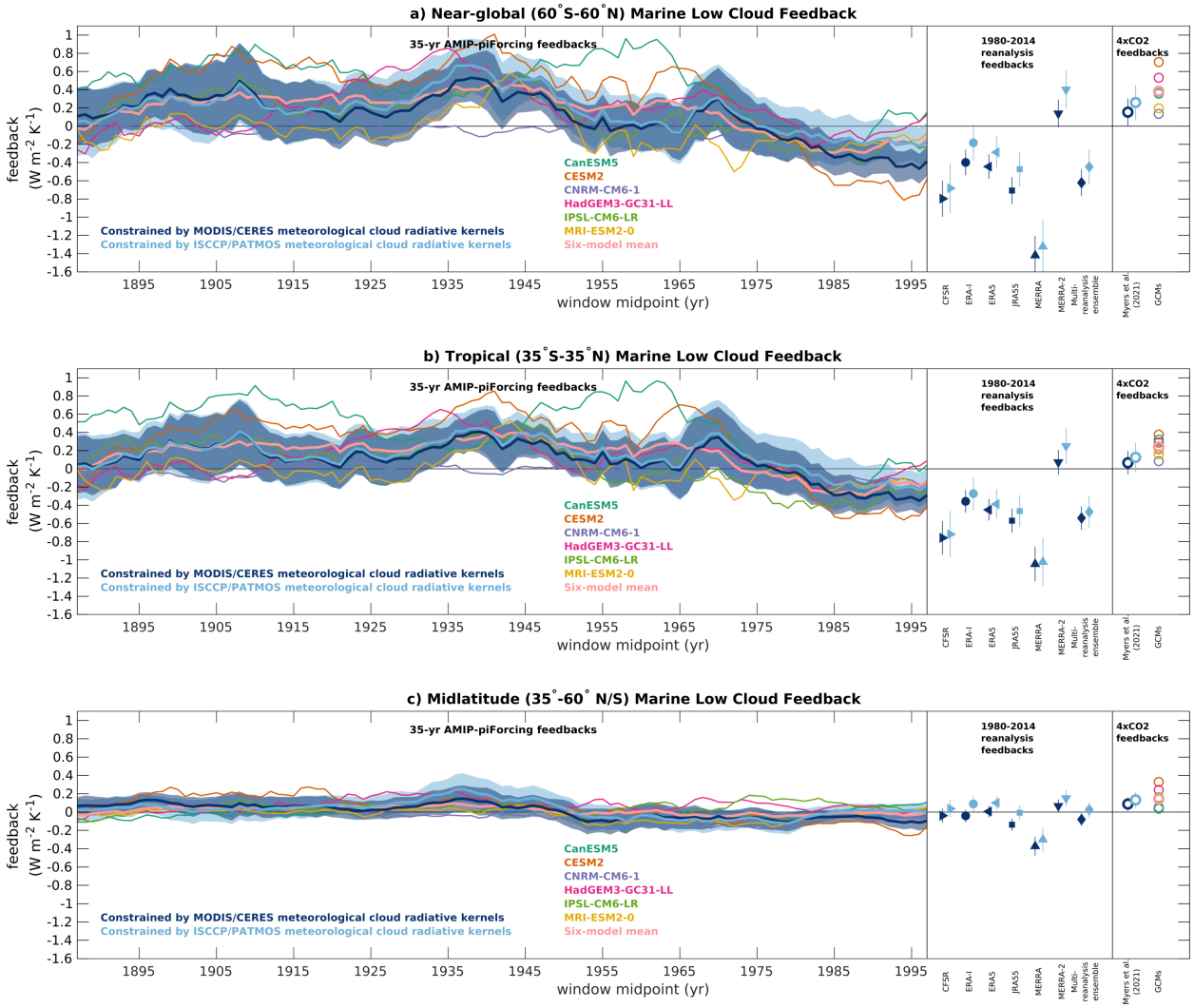

FIG. 3. (a) Near-global (60° S - 60° N), (b) tropical (35° S - 35° N), and (c) midlatitude (35° N/S - 60° N/S) marine low cloud feedbacks constrained using observations (following equation (1)) and as simulated by GCMs. Dark blue lines or symbols correspond to estimates constrained by MODIS- and CERES-derived *meteorological cloud radiative kernels*, while light blue lines or symbols correspond to estimates constrained by ISCCP- and PATMOS-x-derived *meteorological cloud radiative kernels*. Observationally-constrained feedbacks are computed using 35-yr meteorological changes from the *AMIP-piForcing* experiments (dark and light blue time series line plots), 1980-2014 meteorological changes from reanalyses (dark and light blue solid-filled shapes), or long-term meteorological changes from the *abrupt4xCO2* experiments (dark and light blue open-faced circles). Shading or error-bars around observationally-constrained estimates span 90% confidence intervals. Multicolored time series line plots for GCMs correspond to 35-yr feedbacks from the *AMIP-piForcing* experiments. Multicolored open-faced circles for GCMs correspond to long-term feedbacks from the *abrupt4xCO2* experiments. All feedbacks are scaled by planetary fractional area.

Accepted for publication in *Journal of Climate*. DOI 10.1175/JCLI-D-22-0862.1.

covariance with SST explain more than half of the variance of the near-global marine low cloud feedback on multi-decadal timescales (Supplementary Figs. 10 and 11). In turn, variability in near-global marine EIS on multi-decadal timescales is primarily driven by changes in free-tropospheric temperature (Supplementary Fig. 12), consistent with the mechanistic understanding of the pattern effect (Andrews and Webb 2018; Dong et al. 2019; Zhou et al. 2016, 2017).

Figure 4 also provides evidence from reanalyses that a large negative near-global feedback component, primarily driven by increasing EIS in the tropics, has occurred in recent decades, qualitatively consistent with the EIS-driven change inferred from the SST-driven atmosphere-only GCM experiments (see also Supplementary Fig. 2). A small negative feedback component from increasing EIS in the midlatitudes is evident as well. These changes are very different than the small negative tropical marine low feedback component from increasing EIS and positive midlatitude feedback component from decreasing EIS inferred from the *abrupt4xCO2* simulations. This suggests that the processes responsible for the changes in EIS and ensuing marine low cloud changes between 1980 and 2014 are distinct from those associated with a long-term increase in CO_2 alone. In the tropics, these processes are likely related to the La Nina-like shift of the tropical Pacific Ocean, a phenomenon that has been attributed to internal climate variability, aerosol cooling, and/or a transient ocean thermostat response to increasing CO_2 (Heede and Fedorov 2021; Watanabe et al. 2021). In the midlatitudes, these processes may be related to a shift of Pacific decadal variability to its cool phase (Chen et al. 2019) and cooling of the Southern Ocean. The latter may be due to Southern Ocean's large thermal inertia, internal climate variability, Antarctic glacial melt, and/or the Antarctic ozone hole (Hartmann 2022; Kostov et al. 2018; Rye et al. 2020).

In the tropics, the reanalyses also provide evidence that strengthening cold Tadv and WS produced small negative marine low cloud feedback components in recent decades, physically consistent with the observed cool shift of Pacific decadal variability and strengthening of the east-west equatorial Pacific SST gradient and associated Walker Circulation (Fig. 4b). The detection of compounding negative cloud feedbacks in the tropics induced by EIS, Tadv, and WS based on reanalyses is corroborated by the positive covariance terms contributing to the time-varying 35-yr feedbacks. As Supplementary Figs. 10 and 11 reveal, the EIS-Tadv and EIS-WS covariance terms explain 15% and 9-13% of variance of the tropical marine low cloud feedback. In total, we find that EIS and its covariability with other factors explain 69-71% and 75-85% of variance of the 35-yr marine low

Accepted for publication in *Journal of Climate.* DOI 10.1175/JCLI-D-22-0862.1.

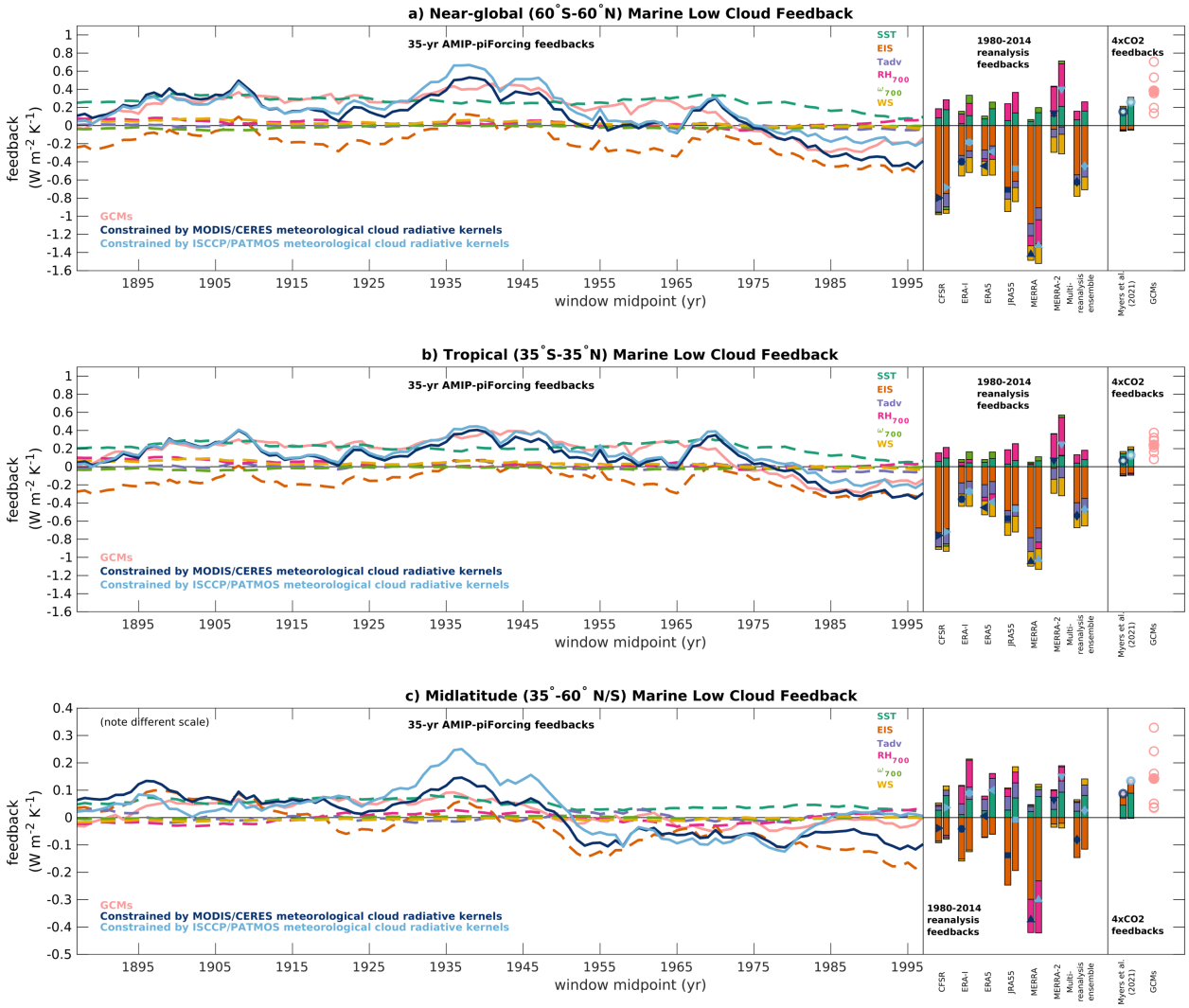

FIG. 4. As in Fig. 3 but also showing individual components of the feedbacks constrained by observations. Each feedback component is associated with a different color dashed line or bar, as indicated in the legend. For example, the orange-colored dashed lines or bars indicate marine low cloud feedbacks driven exclusively by variations in EIS. For clarity, components of feedbacks computed using 35-yr meteorological changes from the *AMIP-piForcing* experiments are only shown for the estimates constrained by MODIS- and CERES-derived *meteorological cloud radiative kernels*. Also for clarity, individual model *abrupt4xCO2* feedbacks are plotted with a single color. Note the different scale of (c), which has been adjusted so that feedback components are clearly visible.

cloud feedback over the tropical and near-global oceans, respectively. This highlights the crucial

Accepted for publication in *Journal of Climate*. DOI 10.1175/JCLI-D-22-0862.1.

role of variations in lower tropospheric stability for generating multi-decadal changes in Earth's energy budget.

We note that there is substantial spread in the feedbacks inferred from reanalysis-based meteorological changes, including a clear outlier, MERRA-2, that predicts positive near-global and tropical marine low cloud feedbacks between 1980 and 2014 (Fig. 3ab and Fig. 4ab). Feedbacks inferred from MERRA, on the other hand, are anomalously negative relative to the other estimates. This demonstrates that climate trends from any single reanalysis may be unreliable. Thus, we advise caution in the use of reanalysis data to investigate cloud feedbacks. Investigations of changes in climate, including clouds, on multi-decadal time scales or longer must consider a variety of reanalysis products and additional sources of evidence (e.g. models, physical understanding, satellite observations) to generate robust results. In our case, we contend that the feedbacks inferred from MERRA-2 are likely in error in light of the results from the other reanalyses and atmosphere-only GCM simulations, observed trends in cloud fraction from multiple datasets, and historical estimates of changes in Earth's radiative budget during the satellite era (Andrews et al. 2022; Clement et al. 2009; Otto et al. 2013; Seethala et al. 2015).

Across-reanalysis covariance matrices of the 1980-2014 marine low cloud feedback components normalized by the across-reanalysis variance of the total feedback itself reveal further insight into the reanalyses (Supplementary Figs. 13 and 14). We find that EIS, RH_{700}, and their covariance explain nearly all of the across-reanalysis variance of the 1980-2014 marine low cloud feedback estimates. In other words, the wide spread of cloud feedbacks inferred from the different reanalyses is overwhelmingly due to uncertainties associated with EIS, RH_{700}, and their covariance. This may be due to the dependence of these CCFs on parameterizations in the models used to generate the reanalyses or to differences in assimilated observing systems among the reanalyses. Improved estimates of these quantities would help to tighten the confidence bounds surrounding marine cloud feedbacks in recent decades.

Accepted for publication in *Journal of Climate.* DOI 10.1175/JCLI-D-22-0862.1.

d. Observationally constraining the pattern effect

We conclude our analysis by observationally constraining the pattern effect. To do so, we define the *cloud feedback pattern effect as*

$$\Delta\lambda_{cloud} = \lambda_{cloud}^{4xCO2} - \lambda_{cloud}^{hist}, \tag{2}$$

where λ_{cloud}^{4xCO2} is the near-global marine low cloud feedback arising from CO_2 quadrupling and λ_{cloud}^{hist} is the near-global marine low cloud feedback over a given historical period, where each feedback has been scaled by planetary fractional area, and where we have omitted the spatial average operator for convenience. This definition follows the methods and sign convention of Sherwood et al. (2020) to compute the pattern effect arising from all climate feedbacks. For λ_{cloud}^{4xCO2} , we use the value constrained by MODIS and CERES and meteorological changes from the *abrupt4xCO2* experiments (as in Myers et al. (2021)). For λ_{cloud}^{hist}, we use values constrained by MODIS and CERES and varying meteorological changes from the *AMIP-piForcing* experiments within 1870-2014 or the 1980-2014 meteorological changes from reanalyses. Our formulation excludes pattern effects from clouds over land and poleward of 60° N/S; we expect these effects to be smaller than those from marine low clouds. Uncertainty of $\Delta\lambda_{cloud}$ is computed by adding uncertainties of λ_{cloud}^{4xCO2} and λ_{cloud}^{hist} in quadrature.

Figure 5 displays $\Delta\lambda_{cloud}$ constrained in this way as a function of all available 35-yr changes in SST and EIS with planetary warming within 1870-2014. The pattern effect depends strongly on time period and reanalysis dataset considered, with changes in SST and EIS explaining much of its variability. Changes in SST and EIS with warming tend to be anti-correlated, and $\Delta\lambda_{cloud}$ increases rapidly as $d\mathrm{SST}/dT_g$ decreases and $d\mathrm{EIS}/dT_g$ increases. Based on the climate changes of recent decades, a strong positive pattern effect is implied, whereas a weaker or even negative pattern effect is implied when earlier decades in the historical period are selected. Furthermore, the reanalysis-based estimates imply vastly different pattern effect magnitudes even when excluding the unrealistic MERRA-2 (from which a near-zero pattern effect is implied), ranging from 0.55 W m^{-2} K^{-1} (ERA-I) to 1.57 W m^{-2} K^{-1} (MERRA) (see also Table 2). Still, our estimates provide observational evidence that the *cloud feedback pattern effect* of recent decades is positive, meaning

Accepted for publication in *Journal of Climate.* DOI 10.1175/JCLI-D-22-0862.1.

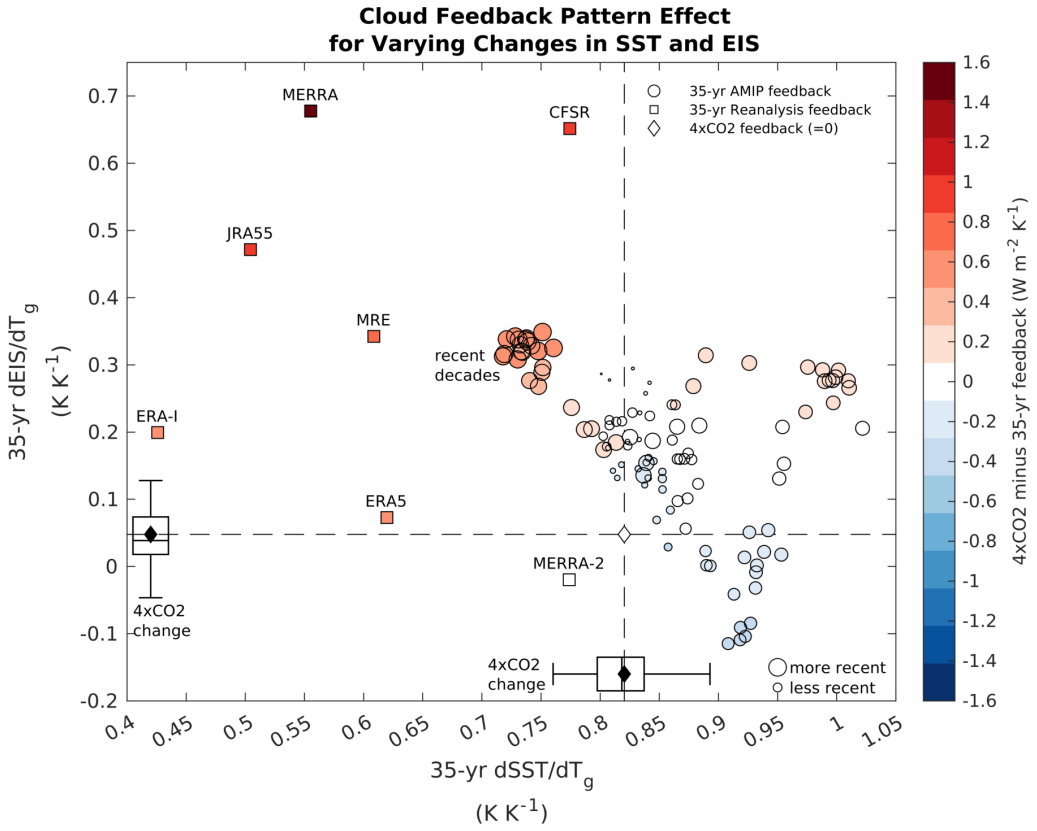

FIG. 5. *Cloud feedback pattern effect*, $\Delta\lambda_{cloud}$, constrained by MODIS- and CERES-derived *meteorological cloud radiative kernels* as a function of all available 35-yr changes in near-global (60° S - 60° N) SST and EIS with planetary warming within 1870-2014, computed using meteorological changes from *AMIP-piForcing* experiments or reanalyses. Increasing circle size corresponds to more recent 35-yr periods. Long-term changes in SST and EIS with planetary warming from *abrupt4xCO2* experiments of the 18 CMIP5 and CMIP6 models considered by Myers et al. (2021) are also shown as box plots, in which the diamond denotes the ensemble mean, the middle line denotes the median, the box spans the interquartile range, and the whiskers span the full range of values. Dashed vertical and horizontal lines representing the ensemble mean *abrupt4xCO2* changes in SST and EIS with planetary warming, respectively, are also plotted for clarity. A *cloud feedback pattern effect* of zero (by definition) is plotted as a diamond at the intersection of these lines for additional reference.

that cloud feedbacks from increasing CO_2 are likely more amplifying than the recent historical feedbacks.

Although we have shown a strong time-dependence of $\Delta\lambda_{cloud}$, we also compute $\Delta\lambda_{cloud}$ using long-term 1870-2014 meteorological changes from the *AMIP-piForcing* experiments. This allows

Accepted for publication in *Journal of Climate*. DOI 10.1175/JCLI-D-22-0862.1.

Table 2. Estimates of the *cloud feedback pattern effect*, $\Delta\lambda_{cloud}$ (in W m^{-2} K^{-1}), and the pattern effect arising from all climate feedbacks, $\Delta\lambda$ (in W m^{-2} K^{-1}), constrained by MODIS- and CERES-derived *meteorological cloud radiative kernels* and 1980-2014 meteorological changes from *AMIP-piForcing* experiments or reanalyses. Error-bars span 90% confidence intervals. Uncertainty in $\Delta\lambda$ is computed by adding uncertainties of $\Delta\lambda_{cloud}$ and $\Delta\lambda_{other}$ in quadrature. Note that for each reanalysis-based $\Delta\lambda_{cloud}$ estimate, error-bars consider uncertainty exclusively arising from imperfect estimates of $\partial R(\theta,\phi)/\partial x_i$.

Dataset for Meteorological Changes	$\Delta\lambda_{cloud}$	$\Delta\lambda$
AMIP-piForcing	0.54±0.22	1.62±0.46
CFSR	0.95±0.25	2.03±0.47
ERA-I	0.55±0.21	1.63±0.45
ERA5	0.60±0.20	1.68±0.45
JRA55	0.86±0.21	1.94±0.45
MERRA	1.57±0.26	2.65±0.48
MERRA-2	0.01±0.22	1.1±0.45
Multi-reanalysis Ensemble	0.78±0.21	1.86±0.45

for a comparison to published estimates of the pattern effect. Here, we compute the meteorological changes per degree planetary warming as the difference in mean x_i divided by the difference in mean T_g between years 1870-1904 (first 35 years) and 1980-2014 (last 35 years), averaged over six models. In this case, $\Delta\lambda_{cloud}$ becomes 0.18±0.22 W m^{-2} K^{-1}, much weaker than values based on the climate changes of recent decades, a finding consistent with Andrews et al. (2022).

To further put our results into the context of previous work, we convert our observationally constrained estimates of the *cloud feedback pattern effect* to estimates of the pattern effect arising from all climate feedbacks, $\Delta\lambda$ (the *abrupt4xCO2* climate feedback parameter, λ, minus the historical λ). We do this as follows. First, we select the long-term GCM-based values of $\Delta\lambda$ provided by Andrews et al. (2022). We also use the methods and data from Andrews et al. (2022) to compute GCM-based values of $\Delta\lambda$ for 1980-2014. For each time period, we then subtract the simulated $\Delta\lambda_{cloud}$ from $\Delta\lambda$ for the six GCMs considered in our study and compute the ensemble mean to derive the portion of the pattern effect, $\Delta\lambda_{other}$, that arises from feedbacks not related to marine low clouds (e.g from changes in lapse rate). Finally, we add this GCM-based quantity and its uncertainty (taken as the inter-model range) to our observationally-constrained estimates of

Accepted for publication in *Journal of Climate.* DOI 10.1175/JCLI-D-22-0862.1.

$\Delta\lambda_{cloud}$ to derive constrained estimates of $\Delta\lambda$, given as

$$\Delta\lambda = \Delta\lambda_{cloud} + \Delta\lambda_{other}. \quad (3)$$

The results for the recent observational period are summarized in Table 2. Using 1980-2014 meteorological changes from the Multi-reanalysis Ensemble, we find that $\Delta\lambda$=1.86±0.45 W m^{-2} K^{-1}, though considerable uncertainty is evident across the reanalysis-based estimates. Using 1870-2014 meteorological changes from the *AMIP-piForcing* experiments, we find that $\Delta\lambda$=0.72±0.28 W m^{-2} K^{-1}. These estimates are similar to and statistically indistinguishable from those derived by Andrews et al. (2022) using GCMs alone (see their Table 3), though we find a somewhat larger value of $\Delta\lambda$ for recent decades. Therefore, independent model and observational evidence suggests that global climate feedbacks associated with increasing CO_2 are more amplifying than historical feedbacks, especially in the last several decades.

4. Conclusions

We have provided observational evidence for the pattern effect using cloud-controlling factor analysis. In this framework, we estimate multi-decadal marine low cloud feedbacks from 1870 to 2014 by convolving the satellite-derived *meteorological cloud radiative kernels* developed by Scott et al. (2020) with estimates of historical meteorological changes with planetary warming. Atmospheric reanalyses and GCMs forced by historical SST patterns provide estimates of the historical meteorological changes. This framework is meant to constrain the response of clouds to large-scale forcing (SST patterns and associated meteorological perturbations), not to reduce the uncertainty surrounding the large-scale forcing itself.

Multi-decadal (35-yr) variations in the low cloud feedback observationally-constrained in this way are qualitatively consistent with variations in cloud feedbacks produced by the ensemble mean of GCMs forced by historical SST patterns. Recent feedbacks are anomalous relative to the previous ~100 years, consistent with previous studies (Andrews et al. 2018, 2022; Dong et al. 2021). Feedbacks constrained by satellite observations and 1980-2014 meteorological changes from reanalyses are strongly negative in the stratocumulus regions over the eastern subtropical Pacific and driven primarily by increasing EIS, similar to feedbacks constrained by 1980-2014 meteorological changes from GCMs forced by historical SSTs. Hence, changes in marine clouds

Accepted for publication in *Journal of Climate.* DOI 10.1175/JCLI-D-22-0862.1.

over the last several decades have likely been driven by changes in the pattern of SST and the resulting variations in large-scale meteorological conditions, primarily an increase in EIS. This corroborates the findings of Zhou et al. (2016) and Cesana and Del Genio (2021). We note that our method does not estimate historical changes in low clouds driven by aerosols alone, which may play a role in the pattern effect (Salvi et al. 2022); this is a topic we leave for future research. For example, the framework of Wall et al. (2022) provides a means to observationally constrain the impact of aerosols on historical marine cloud changes - and, by extension, the pattern effect.

Crucially, long-term marine low cloud feedbacks from increasing CO_2 constrained by observations (as in Myers et al. (2021)) and simulated by GCMs are much more amplifying than the recent historical feedbacks simulated by models or as estimated using our observational approach. This implies a strong pattern effect and suggests that the processes responsible for recent historical marine low cloud changes are distinct from those associated with a long-term increase in CO_2.

However, the *cloud feedback pattern effect* (the difference between the 35-yr historical and long-term CO_2-induced near-global marine low cloud feedbacks) constrained by observations depends strongly on time period and reanalysis dataset considered. Indeed, the pattern effect computed using 1980-2014 meteorological changes from the six out of seven reanalyses that are not obviously in error ranges from 0.55 W m^{-2} K^{-1} (ERA-I) to 1.57 W m^{-2} K^{-1} (MERRA). Additionally, the constrained pattern effect computed using meteorological changes from SST-driven atmosphere-only GCMs implies a near-zero, weak, or pattern effect of opposite sign for several non-recent periods since 1870. We attribute the time- and dataset-dependence of the pattern effect to varying changes in SST and EIS with planetary warming.

We also derived observationally constrained estimates of the pattern effect arising from all climate feedbacks by using GCM simulations to simply add to the *cloud feedback pattern effect* the portion of the pattern effect that arises from feedbacks not related to marine low clouds (e.g. from changes in lapse rate). The resulting estimates are similar to those provided by Andrews et al. (2022), though considerable uncertainty exists owing to the large spread of 1980-2014 meteorological changes across reanalyses.

The observational evidence we have presented bolsters confidence in previous estimates of the pattern effect, which, prior to our work, relied largely upon model estimates of cloud changes. Our findings motivate further study addressing the basic question at the heart of the pattern effect:

Accepted for publication in *Journal of Climate.* DOI 10.1175/JCLI-D-22-0862.1.

Why does the recent historical pattern of Pacific SST change not resemble the SST response to increasing CO_2 predicted by GCMs? The leading hypotheses addressing this question (Hartmann 2022; Heede and Fedorov 2021; Kostov et al. 2018; Rye et al. 2020; Seager et al. 2019; Sherwood et al. 2020; Watanabe et al. 2021; Wills et al. 2022) have different implications for climate sensitivity, which underscores the importance of further reducing this key climate change uncertainty. Our findings also motivate a greater understanding for the reasons behind disparate behavior across reanalyses. We have identified EIS, RH_{700}, and their covariance as the dominant drivers of reanalysis uncertainty. Reducing uncertainty with respect to how SST patterns and associated meteorological perturbations actually evolved over recent decades would help to narrow the bounds of uncertainty surrounding the pattern effect.

Accepted for publication in *Journal of Climate.* DOI 10.1175/JCLI-D-22-0862.1.

Acknowledgments. T.A.M. was supported in part by the NOAA Cooperative Agreement with CIRES, NA17OAR4320101 and NA22OAR4320151, and by the NOAA/ESRL Atmospheric Science for Renewable Energy (ASRE) program. T.A.M., M.D.Z., and S.A.K. worked under the auspices of the United States Department of Energy (DOE), Lawrence Livermore National Laboratory under contract no. DE-AC52-07NA27344 and were supported by the Regional and Global Model Analysis Program of the Office of Science at the DOE. We acknowledge the World Climate Research Programme's Working Group on Coupled Modelling, which is responsible for CMIP, and we thank the climate modelling groups for producing and making available their model output. We also thank the Earth System Grid Federation (ESGF) for archiving the model output and providing access, and we thank the multiple funding agencies who support CMIP and ESGF. We lastly thank Dr. Tim Andrews and two anonymous reviewers for critically assessing our manuscript.

Data availability statement. The *meteorological cloud radiative kernels* applied in this study are freely available for download at `https://github.com/tamyers87/meteorological_cloud_radiative_kernels`. All data used in this work are freely available for download at: `https://modis-atmos.gsfc.nasa.gov/MOD06_L2/index.html` (MODIS), `https://ceres.larc.nasa.gov/data/` (CERES-FBCT), `https://www.ncdc.noaa.gov/isccp/isccp-data-access` (ISCCP), `http://climserv.ipsl.polytechnique.fr/gewexca/instruments/PATMOSX.html` (PATMOS-x), and `https://esgf-node.llnl.gov` (CMIP output and reanalysis data).

References

Andrews, T., and M. J. Webb, 2018: The dependence of global cloud and lapse rate feedbacks on the spatial structure of tropical pacific warming. *Journal of Climate*, **31 (2)**, 641–654.

Andrews, T., and Coauthors, 2018: Accounting for changing temperature patterns increases historical estimates of climate sensitivity. *Geophysical Research Letters*, **45 (16)**, 8490–8499.

Andrews, T., and Coauthors, 2022: On the effect of historical sst patterns on radiative feedback. *Journal of Geophysical Research: Atmospheres*, **127 (18)**, e2022JD036 675.

Bodas-Salcedo, A., and Coauthors, 2011: Cosp: Satellite simulation software for model assessment. *Bulletin of the American Meteorological Society*, **92 (8)**, 1023–1043.

Accepted for publication in *Journal of Climate.* DOI 10.1175/JCLI-D-22-0862.1.

Ceppi, P., and S. Fueglistaler, 2021: The el niño–southern oscillation pattern effect. *Geophysical Research Letters*, **48 (21)**, e2021GL095 261.

Ceppi, P., and P. Nowack, 2021: Observational evidence that cloud feedback amplifies global warming. *Proceedings of the National Academy of Sciences*, **118 (30)**, e2026290 118.

Cesana, G. V., and A. D. Del Genio, 2021: Observational constraint on cloud feedbacks suggests moderate climate sensitivity. *Nature Climate Change*, **11 (3)**, 213–218.

Chen, Y.-J., Y.-T. Hwang, M. D. Zelinka, and C. Zhou, 2019: Distinct patterns of cloud changes associated with decadal variability and their contribution to observed cloud cover trends. *Journal of Climate*, **32 (21)**, 7281–7301.

Clement, A. C., R. Burgman, and J. R. Norris, 2009: Observational and model evidence for positive low-level cloud feedback. *Science*, **325 (5939)**, 460–464.

Dee, D. P., and Coauthors, 2011: The era-interim reanalysis: Configuration and performance of the data assimilation system. *Quarterly Journal of the royal meteorological society*, **137 (656)**, 553–597.

Dong, Y., C. Proistosescu, K. C. Armour, and D. S. Battisti, 2019: Attributing historical and future evolution of radiative feedbacks to regional warming patterns using a green's function approach: The preeminence of the western pacific. *Journal of Climate*, **32 (17)**, 5471–5491.

Dong, Y., and Coauthors, 2021: Biased estimates of equilibrium climate sensitivity and transient climate response derived from historical cmip6 simulations. *Geophysical Research Letters*, **48 (24)**, e2021GL095 778.

Ebita, A., and Coauthors, 2011: The japanese 55-year reanalysis "jra-55": an interim report. *Sola*, **7**, 149–152.

England, M. H., and Coauthors, 2014: Recent intensification of wind-driven circulation in the pacific and the ongoing warming hiatus. *Nature climate change*, **4 (3)**, 222–227.

Eyring, V., S. Bony, G. A. Meehl, C. A. Senior, B. Stevens, R. J. Stouffer, and K. E. Taylor, 2016: Overview of the coupled model intercomparison project phase 6 (cmip6) experimental design and organization. *Geoscientific Model Development*, **9 (5)**, 1937–1958.

Accepted for publication in *Journal of Climate.* DOI 10.1175/JCLI-D-22-0862.1.

Fueglistaler, S., 2019: Observational evidence for two modes of coupling between sea surface temperatures, tropospheric temperature profile, and shortwave cloud radiative effect in the tropics. *Geophysical Research Letters*, **46 (16)**, 9890–9898.

Gates, W. L., and Coauthors, 1999: An overview of the results of the atmospheric model intercomparison project (amip i). *Bulletin of the American Meteorological Society*, **80 (1)**, 29–56.

Gelaro, R., and Coauthors, 2017: The modern-era retrospective analysis for research and applications, version 2 (merra-2). *Journal of climate*, **30 (14)**, 5419–5454.

Gregory, J., T. Andrews, P. Ceppi, T. Mauritsen, and M. Webb, 2020: How accurately can the climate sensitivity to co2 be estimated from historical climate change? *Climate Dynamics*, **54 (1)**, 129–157.

Gregory, J. M., and T. Andrews, 2016: Variation in climate sensitivity and feedback parameters during the historical period. *Geophysical Research Letters*, **43 (8)**, 3911–3920.

Hartmann, D. L., 2022: The antarctic ozone hole and the pattern effect on climate sensitivity. *Proceedings of the National Academy of Sciences*, **119 (35)**, e2207889 119.

Heede, U. K., and A. V. Fedorov, 2021: Eastern equatorial pacific warming delayed by aerosols and thermostat response to co2 increase. *Nature Climate Change*, **11 (8)**, 696–703.

Heidinger, A. K., M. J. Foster, A. Walther, and X. Zhao, 2014: The pathfinder atmospheres–extended avhrr climate dataset. *Bulletin of the American Meteorological Society*, **95 (6)**, 909–922.

Hersbach, H., and Coauthors, 2020: The era5 global reanalysis. *Quarterly Journal of the Royal Meteorological Society*, **146 (730)**, 1999–2049.

Hurrell, J. W., J. J. Hack, D. Shea, J. M. Caron, and J. Rosinski, 2008: A new sea surface temperature and sea ice boundary dataset for the community atmosphere model. *Journal of Climate*, **21 (19)**, 5145–5153.

Kamae, Y., M. Watanabe, T. Ogura, M. Yoshimori, and H. Shiogama, 2015: Rapid adjustments of cloud and hydrological cycle to increasing co 2: A review. *Current climate change reports*, **1**, 103–113.

Accepted for publication in *Journal of Climate.* DOI 10.1175/JCLI-D-22-0862.1.

Klein, S. A., A. Hall, J. R. Norris, and R. Pincus, 2017: Low-cloud feedbacks from cloud-controlling factors: A review. *Shallow clouds, water vapor, circulation, and climate sensitivity*, 135–157.

Kostov, Y., D. Ferreira, K. C. Armour, and J. Marshall, 2018: Contributions of greenhouse gas forcing and the southern annular mode to historical southern ocean surface temperature trends. *Geophysical Research Letters*, **45 (2)**, 1086–1097.

Loeb, N. G., T. J. Thorsen, J. R. Norris, H. Wang, and W. Su, 2018: Changes in earth's energy budget during and after the "pause" in global warming: an observational perspective. *Climate*, **6 (3)**, 62.

Loeb, N. G., and Coauthors, 2020: New generation of climate models track recent unprecedented changes in earth's radiation budget observed by ceres. *Geophysical Research Letters*, **47 (5)**, e2019GL086 705.

Modak, A., and T. Mauritsen, 2022: Better constrained climate sensitivity when accounting for dataset dependency on pattern effect estimates. *EGUsphere [preprint]*, 1–20.

Myers, T. A., C. R. Mechoso, G. V. Cesana, M. J. DeFlorio, and D. E. Waliser, 2018: Cloud feedback key to marine heatwave off baja california. *Geophysical Research Letters*, **45 (9)**, 4345–4352.

Myers, T. A., and J. R. Norris, 2015: On the relationships between subtropical clouds and meteorology in observations and cmip3 and cmip5 models. *Journal of Climate*, **28 (8)**, 2945–2967.

Myers, T. A., R. C. Scott, M. D. Zelinka, S. A. Klein, J. R. Norris, and P. M. Caldwell, 2021: Observational constraints on low cloud feedback reduce uncertainty of climate sensitivity. *Nature Climate Change*, **11 (6)**, 501–507.

Norris, J. R., and A. T. Evan, 2015: Empirical removal of artifacts from the isccp and patmos-x satellite cloud records. *Journal of Atmospheric and Oceanic Technology*, **32 (4)**, 691–702.

Otto, A., and Coauthors, 2013: Energy budget constraints on climate response. *Nature Geoscience*, **6 (6)**, 415–416.

Accepted for publication in *Journal of Climate.* DOI 10.1175/JCLI-D-22-0862.1.

Pincus, R., S. Platnick, S. A. Ackerman, R. S. Hemler, and R. J. P. Hofmann, 2012: Reconciling simulated and observed views of clouds: Modis, isccp, and the limits of instrument simulators. *Journal of Climate*, **25 (13)**, 4699–4720.

Potter, G. L., L. Carriere, J. Hertz, M. Bosilovich, D. Duffy, T. Lee, and D. N. Williams, 2018: Enabling reanalysis research using the collaborative reanalysis technical environment (create). *Bulletin of the American Meteorological Society*, **99 (4)**, 677–687.

Qu, X., A. Hall, S. A. Klein, and P. M. Caldwell, 2015: The strength of the tropical inversion and its response to climate change in 18 cmip5 models. *Climate Dynamics*, **45**, 375–396.

Rayner, N., D. E. Parker, E. Horton, C. K. Folland, L. V. Alexander, D. Rowell, E. C. Kent, and A. Kaplan, 2003: Global analyses of sea surface temperature, sea ice, and night marine air temperature since the late nineteenth century. *Journal of Geophysical Research: Atmospheres*, **108 (D14)**.

Reynolds, R. W., N. A. Rayner, T. M. Smith, D. C. Stokes, and W. Wang, 2002: An improved in situ and satellite sst analysis for climate. *Journal of climate*, **15 (13)**, 1609–1625.

Rienecker, M. M., and Coauthors, 2011: Merra: Nasa's modern-era retrospective analysis for research and applications. *Journal of climate*, **24 (14)**, 3624–3648.

Rye, C. D., J. Marshall, M. Kelley, G. Russell, L. S. Nazarenko, Y. Kostov, G. A. Schmidt, and J. Hansen, 2020: Antarctic glacial melt as a driver of recent southern ocean climate trends. *Geophysical Research Letters*, **47 (11)**, e2019GL086 892.

Saha, S., and Coauthors, 2010: The ncep climate forecast system reanalysis. *Bulletin of the American Meteorological Society*, **91 (8)**, 1015–1058.

Salvi, P., P. Ceppi, and J. M. Gregory, 2022: Interpreting differences in radiative feedbacks from aerosols versus greenhouse gases. *Geophysical Research Letters*, **49 (8)**, e2022GL097 766.

Scott, R. C., T. A. Myers, J. R. Norris, M. D. Zelinka, S. A. Klein, M. Sun, and D. R. Doelling, 2020: Observed sensitivity of low-cloud radiative effects to meteorological perturbations over the global oceans. *Journal of Climate*, **33 (18)**, 7717–7734.

Accepted for publication in *Journal of Climate.* DOI 10.1175/JCLI-D-22-0862.1.

Seager, R., M. Cane, N. Henderson, D.-E. Lee, R. Abernathey, and H. Zhang, 2019: Strengthening tropical pacific zonal sea surface temperature gradient consistent with rising greenhouse gases. *Nature Climate Change*, **9 (7)**, 517–522.

Seethala, C., J. R. Norris, and T. A. Myers, 2015: How has subtropical stratocumulus and associated meteorology changed since the 1980s? *Journal of Climate*, **28 (21)**, 8396–8410.

Sherwood, S., and Coauthors, 2020: An assessment of earth's climate sensitivity using multiple lines of evidence. *Reviews of Geophysics*, **58 (4)**, e2019RG000 678.

Silvers, L., and S. Fueglistaler, 2021: The peculiar trajectory of global warming. *Journal of Geophysical Research: Atmospheres*, **126 (4)**, e2020JD033 629.

Silvers, L. G., D. Paynter, and M. Zhao, 2018: The diversity of cloud responses to twentieth century sea surface temperatures. *Geophysical Research Letters*, **45 (1)**, 391–400.

Sun, M., D. R. Doelling, N. G. Loeb, R. C. Scott, J. Wilkins, L. T. Nguyen, and P. Mlynczak, 2022: Clouds and the earth's radiant energy system (ceres) fluxbycldtyp edition 4 data product. *Journal of Atmospheric and Oceanic Technology*, **39 (3)**, 303–318.

Taylor, K. E., D. Williamson, and F. Zwiers, 2000: *The sea surface temperature and sea-ice concentration boundary conditions for AMIP II simulations*. Program for Climate Model Diagnosis and Intercomparison, Lawrence Livermore National Laboratory.

Wall, C. J., J. R. Norris, A. Possner, D. T. McCoy, I. L. McCoy, and N. J. Lutsko, 2022: Assessing effective radiative forcing from aerosol–cloud interactions over the global ocean. *Proceedings of the National Academy of Sciences*, **119 (46)**, e2210481 119.

Watanabe, M., J.-L. Dufresne, Y. Kosaka, T. Mauritsen, and H. Tatebe, 2021: Enhanced warming constrained by past trends in equatorial pacific sea surface temperature gradient. *Nature Climate Change*, **11 (1)**, 33–37.

Webb, M. J., and Coauthors, 2006: On the contribution of local feedback mechanisms to the range of climate sensitivity in two gcm ensembles. *Climate dynamics*, **27 (1)**, 17–38.

Webb, M. J., and Coauthors, 2017: The cloud feedback model intercomparison project (cfmip) contribution to cmip6. *Geoscientific Model Development*, **10 (1)**, 359–384.

Accepted for publication in *Journal of Climate.* DOI 10.1175/JCLI-D-22-0862.1.

Wills, R. C., Y. Dong, C. Proistosecu, K. C. Armour, and D. S. Battisti, 2022: Systematic climate model biases in the large-scale patterns of recent sea-surface temperature and sea-level pressure change. *Geophysical Research Letters*, **49 (17)**, e2022GL100 011.

Young, A. H., K. R. Knapp, A. Inamdar, W. Hankins, and W. B. Rossow, 2018: The international satellite cloud climatology project h-series climate data record product. *Earth System Science Data*, **10 (1)**, 583–593.

Zelinka, M. D., S. A. Klein, and D. L. Hartmann, 2012: Computing and partitioning cloud feedbacks using cloud property histograms. part i: Cloud radiative kernels. *Journal of Climate*, **25 (11)**, 3715–3735.

Zelinka, M. D., T. A. Myers, D. T. McCoy, S. Po-Chedley, P. M. Caldwell, P. Ceppi, S. A. Klein, and K. E. Taylor, 2020: Causes of higher climate sensitivity in cmip6 models. *Geophysical Research Letters*, **47 (1)**, e2019GL085 782.

Zhao, X., and R. J. Allen, 2019: Strengthening of the walker circulation in recent decades and the role of natural sea surface temperature variability. *Environmental Research Communications*, **1 (2)**, 021 003.

Zhou, C., M. D. Zelinka, and S. A. Klein, 2016: Impact of decadal cloud variations on the earth's energy budget. *Nature Geoscience*, **9 (12)**, 871–874.

Zhou, C., M. D. Zelinka, and S. A. Klein, 2017: Analyzing the dependence of global cloud feedback on the spatial pattern of sea surface temperature change with a g reen's function approach. *Journal of Advances in Modeling Earth Systems*, **9 (5)**, 2174–2189.

Zhou, X., J. Zhang, and G. Feingold, 2021: On the importance of sea surface temperature for aerosol-induced brightening of marine clouds and implications for cloud feedback in a future warmer climate. *Geophysical Research Letters*, **48 (24)**, e2021GL095 896.

Accepted for publication in *Journal of Climate.* DOI 10.1175/JCLI-D-22-0862.1.